Journal of Manufacturing Processes 104 (2023) 218–229

Contents lists available at ScienceDirect

Journal of Manufacturing Processes

journal homepage: www.elsevier.com/locate/manpro

BRDF representation in response to the build orientation in 3D-printed digital materials

Ali Payami Golhin [a,*], Aditya Suneel Sole [b], Are Strandlie [a]

[a] Department of Manufacturing and Civil Engineering, NTNU - Norwegian University of Science and Technology, 2815 Gjøvik, Norway
[b] Department of Computer Science, Norwegian University of Science and Technology, 2815 Gjøvik, Norway

ARTICLE INFO

Keywords:
Bidirectional reflectance distribution function
Spectral analysis
Digital materials
Appearance
3D printing

ABSTRACT

Additively manufactured (AM) parts still lack a thorough understanding of their optical properties, particularly surface texture and reflectance characteristics at different viewing angles. This study examines the reflectance properties of material jetting (MJT) parts using bidirectional reflectance distribution functions (BRDFs). The visual appearance of the MJT parts was analyzed using a gonio-spectrophotometer at 328 unique incidence and viewing geometries for seven different wedge angles for build orientation (BO) from 0° to 90° at 15° intervals. The redundancy analysis (RDA) and principal component analysis (PCA) were used to study BO and to determine the prominent measurement geometries. The results indicate higher BOs resulted in more color and texture variation and rougher surfaces, with S_q 4.21 μm vertical compared to 1.42 μm for horizontal BOs. Furthermore, it affected the visual representation and parametric estimation of BRDF, where significantly lower luminance, more diffuse reflection, and less hue distribution were observed for all CMYK resins printed at higher BOs. Accordingly, vertically printed surfaces showed a wider near-to-specular luminance area than other BOs. An analysis of the bidirectional reflectance property suggests that a gonio-spectrophotometer can be embedded in the printing process and quality assurance in AM as a computationally efficient model.

1. Introduction

A key advantage of additive manufacturing (AM) is the ability to create complex geometries and customized designs. 3D printing in color has become increasingly popular as a result of its ability to produce realistic and vibrant appearances [1]. However, the poor surface finish and high roughness of 3D-printed models have limited the widespread adoption of this technology and require additional post-processing for most applications [2]. Moreover, it is challenging to achieve accurate color reproduction due to the complex interaction of light with the surface, particularly when measuring 3D-printed polymers. Typically, this is due to their structural color, translucency, and high gloss appearance [3,4], which affects the perception of color. Structure color refers to the color produced by light interference, diffraction, and scattering on the surface microstructure of a material [5]. Using an optimized AM method to reduce the inherent roughness of the surface can also affect the appearance of structured AM surfaces [2]. To ensure quality control and to meet the color 3D printing expectations, it is essential to accurately measure the appearance attributes of 3D printed parts.

Material jetting (MJT) techniques, such as PolyJet, have become popular in producing functional polymers, scaffolds for tissue engineering, multi-material structures, and memory shape polymers for 4D printing [6,7]. It is primarily due to their general homogeneity and accuracy [8]. Furthermore, MJT with a typical average surface roughness of $R_a < 10$ μm is a promising technology for 3D printing smooth surfaces as it can be considered in the range between vat photopolymerization ($R_a < \sim 5$ μm) and fused filament fabrication (~ 1 μm $< R_a < \sim 35$ μm)

Abbreviations: AM, Additive manufacturing; BO, Build orientation; BRDF, Bidirectional reflectance distribution function; BSSRDF, Bidirectional scattering-surface reflectance distribution function; BTDF, Bidirectional transmittance distribution function; CIE, Commission Internationale de l'éclairage; CMYK, Cyan, Magenta, Yellow, and Black colors; FDM, Fused deposition modeling; GoG, Glossy-on-Glossy finish; MJT, Material jetting; PC, Principal component; PCA, Principal component analysis; RDA, Redundancy analysis; S_a, Height deviations from the mean reference plane of the measurement area; SD, Standard deviation; S_{ku}, Kurtosis; S_q, Root mean square of surface heights; sRGB, Standard RGB (red, green, blue); S_{sk}, Skewness; svBRDF, spatially varying BRDF; θ_i, Incident angle; θ_r, Viewing angle; $\theta_{r\text{-}S}$, Specular reflection angle.

* Corresponding author.
E-mail address: ali.p.golhin@ntnu.no (A.P. Golhin).

https://doi.org/10.1016/j.jmapro.2023.09.016
Received 24 March 2023; Received in revised form 20 August 2023; Accepted 5 September 2023

[2]. Despite the popularity of 2D profile measurements using a stylus, there is a growing interest in X-ray computed tomography (CT) scanning (ISO 4287) and contactless 3D optical profilometry (ISO 25178–2) to obtain greater information without scratching the surface [2]. However, more studies are required to adopt a non-destructive method for assessing both the surface roughness and visual appearance of the same AM specimen due to their translucency in polymers and structured surfaces in 3D-printed parts.

The quality of a printed part can be affected by a number of parameters throughout the printing process. The primary processing parameters, such as layer thickness, printing speed, printing temperature, and feedstock materials, are among the most investigated factors [2,9]. To discuss how these parameters can be optimized to improve surface quality for appearance, it is necessary to examine the role of measurement in appearance assessment. A variety of interactions determine the appearance of an object, including reflection, scattering, and absorption [10]. There is a shortage of accurate color measurement methods, such as spectrophotometry, that can capture these characteristics.

The color of a material is determined by wavelength-specific light phenomena, while the gloss, translucency, and similar properties are determined by geometric or directional selectivity [11]. Numerical expressions of appearance attributes are essential for simplifying quantification and advancing the science and technology of the material appearance field [12]. However, the measurement geometry and direction play a significant role in evaluating the material appearance [11,13].

Material jetting is characterized by the longitudinal stacking effect, which occurs during the layer-by-layer deposition of the material. The longitudinal height variation of printed color samples was taken into account by Wang et al. [14] in developing an evaluation system that differs fundamentally from the current color reproduction quality evaluation system used in graphic printing from the perspective of assessing the geometric characteristics of the printed object.

Among the factors that influence the light reflectance and color appearance of the ink are its spectral characteristics, the thickness of the layer [3,15], the density of the ink, and the surface roughness of structured surfaces [5,10]. To understand the relationship between CMYK colors, light interaction, and the resulting color perception in MJT parts, it is necessary to understand these fundamental principles.

To solve the complexity of appearance measurement in 3D printed parts, various color data analysis categories have emerged in recent years for color reproduction. As reviewed by Yuan et al. [1], the main color reproduction methods include optical parameter modeling, colorimetric difference evaluating, computer-aided colorization, and voxel droplet jetting. By analyzing the captured spectral data and tristimulus values and using CIE Geometries of illumination and measurement [16], these methods are able to extract meaningful information relating to appearance reproduction. Their purpose is to bridge the gap between color measurement and accurate color reproduction in 3D printing.

It is essential to distinguish between the measurement of color and the measurement of color appearance. In color measurement, spectral data for calculating hue, chroma, and lightness are typically measured using objective instruments, such as spectrophotometers, as shown in our previous work [15]. Alternatively, color appearance measurement considers other appearance attributes, such as glossiness, texture, and translucency, to capture a better perception of appearance [3].

In order to address the challenges involved in the measurement of color in 3D printed parts, researchers [17–19] have examined the parameters of the bidirectional reflectance distribution function (BRDF). The BRDF describes the direction in which light is reflected from a surface. It is possible to understand and predict the color appearance of 3D printed materials by characterizing the BRDF parameters [1]. BRDF modeling can be computationally efficient [10] and a reliable appearance assessment method for homogenous and opaque surfaces.

The parameters used in a BRDF model can vary depending on the specific formulation, but common examples include the incident zenith angle (θ_i), which is the angle between the incident light direction and the surface normal, as well as the reflected zenith angle (θ_r), which is the angle between the reflected light direction and the surface normal [20]. Additionally, the incident azimuth angle (φ_i) represents the azimuthal angle in the plane of incidence, while the reflected azimuth angle (φ_r) represents the azimuthal angle in the reflection plane. These parameters establish the geometric relationship between the incident and reflected light directions for a given combination of angles. With the adjustment of these parameters, the BRDF model can accurately represent various reflection behavior types, including diffuse, specular, and anisotropic reflections [21]. For instance, Kumar et al. [22] analyzed surface texture using machine vision by analyzing reflections from a real surface using 3D reconstructions based on anisotropic parametric BRDFs.

Other modeling methods include spatially varying BRDF (svBRDF) [23], or the bidirectional scattering-surface reflectance distribution function (BSSRDF) [24], depending on the optical properties [21]. BSSRDF and svBRDF are considered to be more reliable methods for non-opaque and non-homogenous materials [25]. However, for applications such as on-line quality assurance for 3D-printed products, the BRDF model is significantly faster and simpler to implement than the svBRDF and BSSRDF models, given its reduced dimensionality [26]. MJT surfaces are typically printed smooth and can be glossy [15]. As a result, the BRDF model can be suitable for simulating surface reflectance for MJT surfaces with specular reflections.

There are even more complex models for appearance evaluation based on reflation. The geometric aspect of parts is supposed to affect their aesthetics and perceived quality. An aesthetic quality index (AQI) was developed to evaluate the user-perceived quality of 3D printed parts and their robustness by Galati and Minetola [27]. Serrano et al. [28] presented a model for the effects of shape and illumination on material perception, focusing on six critical dimensions of appearance: glossiness, sharpness of reflections, contrast of reflections, lightness, metallicness, and anisotropy. They demonstrated the ability of the predictor to reproduce gloss in 3D printing based on BRDF editing by integrating the predictor into a differentiable renderer. Accordingly, BRDF can employ accurate physical-based reflectance models to study light interactions with materials by incorporating the surface properties of the material, such as the bidirectional reflectance distribution [29]. For ease of integration, however, reducing the number of parameters describing the BRDF model is necessary.

Several measurement techniques, such as a gonio-reflectometer [30], a dome-shaped system [31], robotic arms integrated with cameras, or an image-based system [32], have been used in the past to measure surface reflectance bidirectionally. However, the process of bidirectional reflectance measurement can also be time-consuming and tedious [1], which requires workflow improvement. Color science and colorimetry widely use the CIEXYZ tristimulus values [16] that are calculated using the surface reflectance, the CIE color-matching function, and spectral power distribution of the light source. The CIEXYZ – Y component represents luminance, an essential aspect of AM color reproduction and color-matching surfaces. The chromaticity coordinates are represented by the CIEXYZ – X and CIEXYZ – Z components [4]. BRDF modeling is heavily influenced by the luminance of the color [13,30]. Although the L* component in the CIELAB and CIELCH color models reflects the lightness of the color [4], this component is based on a nonlinear transformation using the CIEXYZ – Y and therefore is used to model surface reflectance in most of the cases [16,33].

Typical MJT machines such as PolyJet J750 follow a three-dimensional Cartesian coordinate system equipped with a multi-nozzle printhead [34]. The rotary continues manufacturing using recently developed machines, such as Stratasys J55 [15] can produce even more visually appealing 3D objects due to their stability to create homogeneous surfaces. However, MJT is prone to missing/clogged nozzles and depressions (sunken-in areas on the model surface). While routine maintenance and process optimization should cause high reproducibility in part fabrication, by reducing the influence of errors in the

measurement process and following a reproducible procedure, satisfactory results for modeling and application such as multi-materials tissue-mimicking [35] can be achieved.

The build orientation (BO) and the wedge angle for tilted surfaces are considerably flexible, but specific directions may be required depending on the design and to control the surface texture [36,37]. Furthermore, a wrong orientation and high speeds can also impair accuracy and functionality [38–40]. In terms of how BO influences the functionality and quality of MJT parts, limited research is available [41–44] that focuses on the typical MJT machines with Cartesian systems. Nevertheless, the role of rotary discs in studying BRDFs has not yet been addressed.

In this paper, we discuss the role of measurement in appearance assessment using BRDF and color variation models. A detailed analysis of the influence of the build orientation on the MJT surface reflectance is also provided. As part of explaining the role of BO in the surface reflectance model, the variation in the surface texture and roughness in the manufactured parts produced with CMYK resins is discussed as well. The findings are summarized by providing multivariate statistical score results for the most crucial measurement geometries.

2. Methodology

2.1. Test samples and bidirectional surface reflectance measurement

A J55 PolyJet 3D printer (Stratasys, Israel) was employed to generate test samples using VeroCyan, VeroMagenta, VeroYellow, and VeroBlackPlus, as corresponding CMYK colors according to Fig. 1. Vero materials are composed of acrylic oligomers combined with proprietary components, providing low-viscosity materials with similar mechanical, thermal, and electrical properties [45]. Bilayer structures of 35.5 × 40.0 (mm) were constructed using 1 mm thick CMYK plates on a 1 mm thick white background following the best practices of Stratasys for PolyJet and Pantone's guidelines for color-matching [46]. An array of seven different build orientations was printed at intervals of 15° from 0° (reference) to 90° on the middle swath of a rotary disc using a glossy-on-glossy (GoG) finish. To collect data, experiments were designed with a full factorial approach.

Fig. 2a represents specimens manufactured at BO (α) 0°,15°, 75°, and 90° as viewed at 45° and under standard daylight illumination. Bidirectional reflectance was measured spectrally using the GON 360 goniometer (Instrument Systems, Germany) equipped with a CAS 140CT array spectrophotometer (Instrument Systems, Germany). Fig. 2b and c depict the geometry of measurements and the main components of the measurement equipment. Bidirectional spectral reflectance was captured in the 380 nm to 780 nm range at 5 nm intervals and at 328 unique pairs of the incident (θ_i) and viewing (θ_r) directions as measurement geometries. Incidence angles were set between −60° and 0°, and the bidirectional reflectance at viewing angles between −30° and 65° was measured at intervals of 1° for specular and near-to-specular angles and 5° for the rest.

CIEXYZ tristimulus values were further calculated based on the spectral reflectance of the sample surface $S(\lambda)$, D50 illuminant $I(\lambda)$, and CIE standard observer (2°) $\bar{x}$, $\bar{y}$, and $\bar{z}$ color-matching functions according to CIE15.2 [11].

A Keyence VH-ZST microscope (Keyence International, Belgium) was used to non-destructively evaluate the surface morphology and roughness measurements of the 3D-printed objects.

2.2. Redundancy and principal component analysis

Redundancy analysis (RDA) was set to use θ_i and θ_r as observed variables, as well as BOs associated with build orientation as

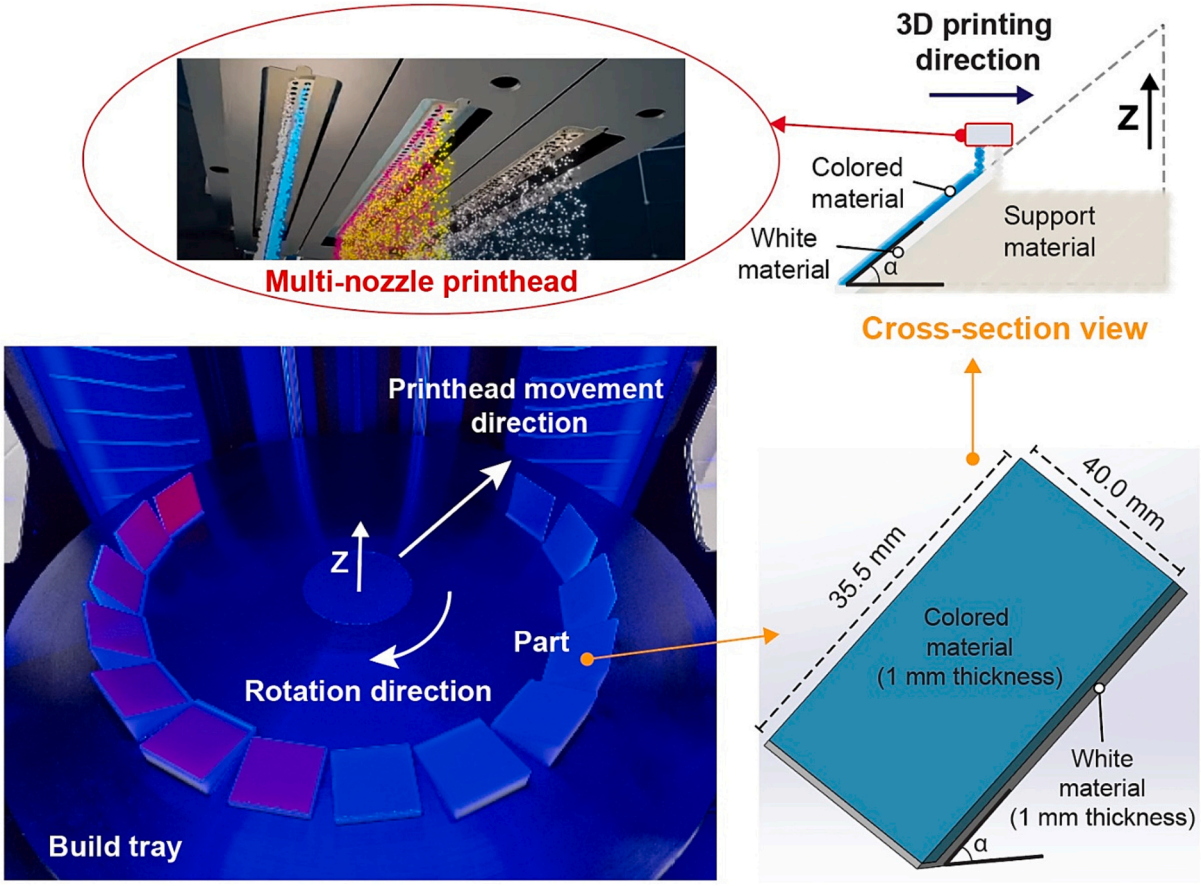

Fig. 1. Manufactured MJT parts using PolyJet technology with a rotating build tray and multi-nozzle printhead. α represents the wedge angle in build orientation.

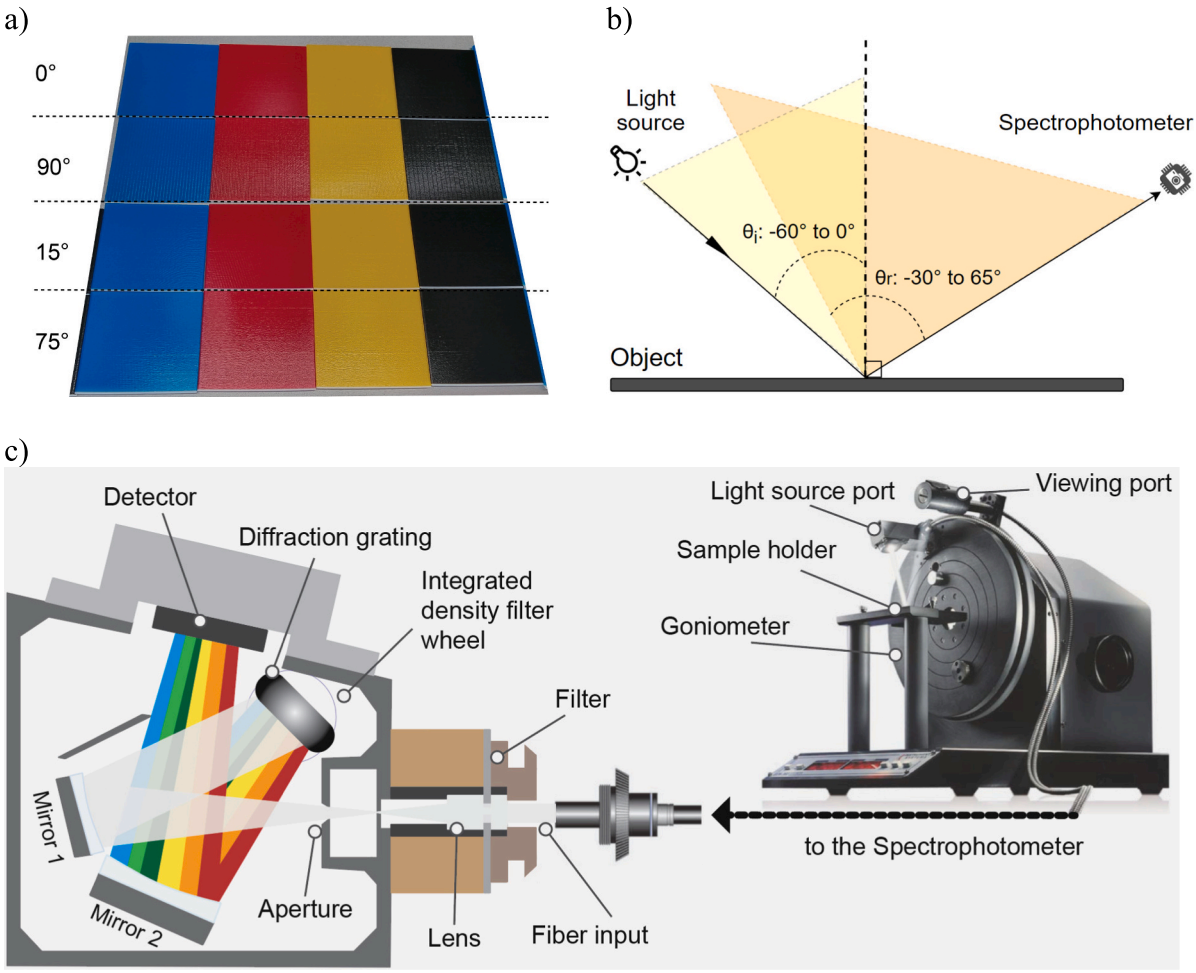

Fig. 2. a) CMYK specimens manufactured at BO 0°,15°, 75°, and 90°, as observed under D50 daylight standard illumination, b) measurement geometries, and c) gonio-spectrophotometer components.

explanatory labels. To validate luminance evaluation by reflectance data and determine the prominent measurement angles, principal component analysis (PCA) was used to analyze multivariate spectral data. PCAs were performed for all 328-reflectance data of each printed resin at different build orientations, considering the correlation matrix. The periodic peaks of pulse integration results for PCA scores were used to identify the most important spectral bands or wavelengths contributing to the observed changes in the Y value as a function of build orientation. Identifying significant wavelengths and frequencies in the spectra resulted in detecting critical BRDF measurement angles. Data analysis was conducted using R statistical software 4.2.1 and Origin 2022 (OriginLab).

3. Results and discussions

CIE1976 u', v' chromaticity diagrams in Fig. 3 show the distribution of 328 points corresponding to the measurement geometries for each CMYK color at various build orientations according to their corresponding BOs in the specimens. Results indicate that when the samples were manufactured at the horizontal direction (BO 0°), there was generally a higher distribution of points for each CMYK color than for higher angles, particularly 90°. Furthermore, the distribution was more pronounced for cyan and magenta colors as compared to black, where yellow resin showed a mediate distribution.

As CMYK colors interact with light at different angles, the distribution of points on the CIE1976 u', v' chromaticity diagram altered. As a result, the distribution of points on the chromaticity diagram will vary. A surface can reflect, absorb, or transmit light, depending on the surface properties. For instance, a smooth and reflective surface may predominantly reflect light, resulting in a glossy appearance. In contrast, a rough surface may scatter and diffuse light in various directions, resulting in a matte or diffused appearance [16]. As a result of the interaction between light and surface properties, the color, glossiness, texture, and other visual characteristics of a surface are determined.

It is common for MJT objects to be complicated in appearance and to represent a mixture of textures created by applying layers of ink [1]. As a result, it is crucial to study the detailed texture properties of the 3D-printed surfaces when evaluating BRDF models using non-invasive and robust surface texture evaluation tools. According to Fig. 4a, the microsurfaces of 3D-printed objects with zero BOs reflect light directly, which may interact for a more extended period and more directly. It led to more scattering of light, thus resulting in a high variation of u' and v' values in the CIE1976 u', v' chromaticity diagram for each CMYK color. Furthermore, it resulted in texture variation, as can be seen in Fig. 4b. With the increasing BO, the microsurfaces of the 3D-printed object were oriented away from the direction of the light source. As a result, light scattering was reduced, resulting in a slight variation of u' and v' values in the CIE1976 u', v' chromaticity diagram. The scattering of the reflected light was higher for cyan and magenta compared to the black material. Therefore, adjusting the object orientation or modifying the resin properties might need to be considered to achieve a more consistent color distribution in MJT.

As listed in Table 1, MJT produced exceptionally smooth surfaces, although it was affected by the build orientation. The smoothest surface

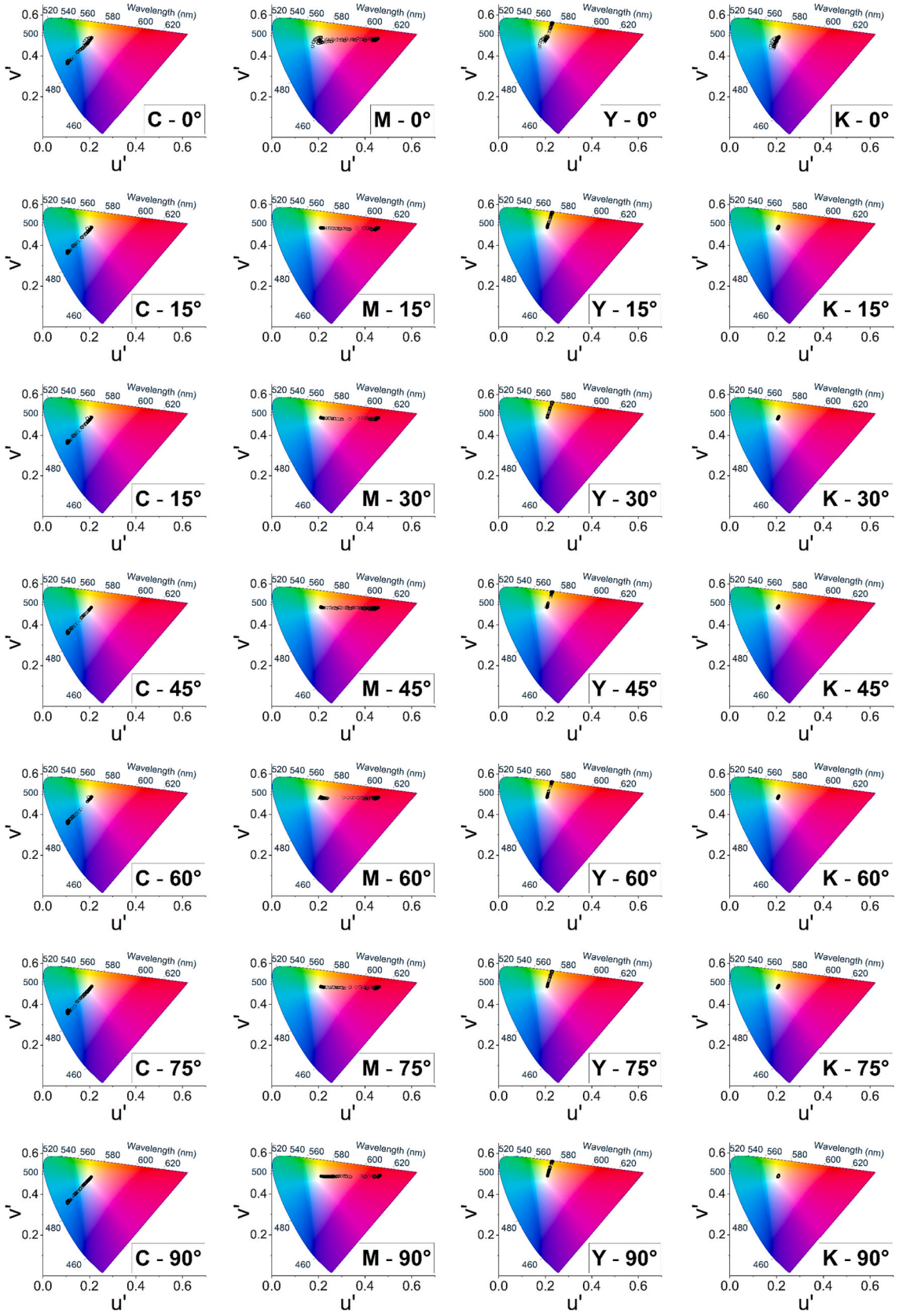

Fig. 3. Hue u', v' stimuli distribution according to CIE1976 chromaticity diagram. C: Cyan, M: Magenta, Y: Yellow, and K: Black. (For interpretation of the references to color in this figure legend, the reader is referred to the web version of this article.)

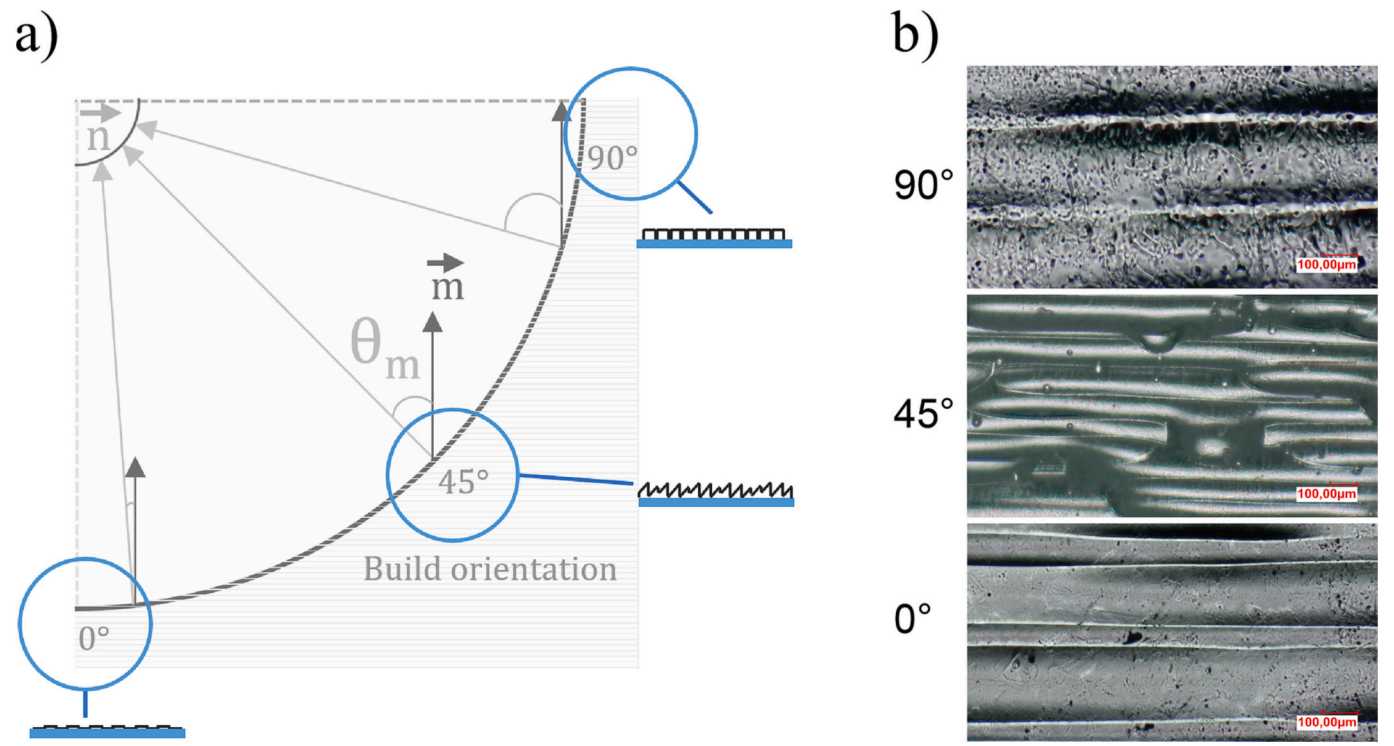

Fig. 4. a) Variation in the surface texture with the build orientation and b) focal microscopic images of BO 0°,45°, and 90°.

Table 1
Results of mean surface roughness.

	Area roughness parameter[a]			
Build orientation (°)	S_a (µm)	S_q (µm)	S_{sk}	S_{ku}
0	1.02	1.42	0.03	2.20
45	2.09	2.65	0.05	3.13
90	3.83	4.21	0.06	2.95

[a] S_a: height deviations from the mean reference plane of the measurement area (A); S_q: root mean square of surface heights.

was obtained with a flat orientation (S_a = 1.02 µm), followed by a BO 45° angle (S_a = 2.09 µm) and a vertical angle (S_a = 3.83 µm). The results are consistent with those reported by Pandey et al. [47] (R_a: 0.818–4.024 µm) and Gülcan et al. [48] (R_a: 0.03–13.59 µm) for other MJT machines, while they measured 2D profiles based on tactile profilometry. All specimens had slightly positive skewness values (S_{sk}), resulting in more peaks and asperities than valleys, according to ISO 25178-2 [49]. These profile peaks were slightly sharp, as indicated by high kurtosis (S_{ku}) values.

As a result of multilayering semi-transparent digital materials to achieve desired aesthetics, MJT objects tend to appear glossy and hazy [50], which can be explained by studying the specular and near-to-specular measurement angles, i.e., at most 10° away from specular reflection ($\theta_{r\text{-}S}$) [30]. A specular reflection occurs when light reflects off a surface at an angle equal to its angle of incidence, resulting in a bright, mirror-like reflection [29]. Y values differ between specular and near-to-specular angles due to differences in reflectance properties. A near-to-specular reflection occurs when light is reflected off a surface at an angle slightly different from the angle of incidence, which results in a diffuse reflection [11]. As evident from the test results in Fig. 5, certain angles showed higher luminances, suggesting that the optical properties at these angles were more efficient at reflecting light and were specular. It provides information about the surface gloss and reflectance of the printed material, which can be correlated with its underlying physical properties, e.g., texture.

Fig. 6 illustrates that the Y component of the tristimulus color value for 3D-printed objects was the maximum for specular angles and decreased as the build orientation increased. In particular, the Y values for specular angles were consistently higher and narrower than those for near-to-specular angles, with maximum values observed at BO 0°. The Y values for both specular and near-to-specular angles decreased with increasing BOs, with a more significant decrease in specular angles. Moreover, BO 90° demonstrated significantly more hazy luminance compared to other specimens for all resins, leading to a complex visual appearance. It was attributed to the change in surface texture and reflectance properties of the printed objects (Fig. 4b). As the wedge angle for BO increased, the surface texture became rougher (Table 1), leading to an increase in diffuse reflection, a decrease in specular reflection, and reducing the Y values. The comprehensive results for the complete list of BO angles and CMYK colors are presented in Appendix A.

Parts printed in a horizontal orientation resulted in smooth surfaces because layers of material were deposited on top of each other. Conversely, the materials were deposited at an angle when pieces were printed in a non-horizontal orientation, i.e., tilted surfaces. It caused stair-stepping effects and a rougher surface finish, resulting in a diffuse appearance [51]. However, several other factors could affect the surface finish of parts produced by MJT, such as the size of the droplets and the duration of the curing process. For instance, reducing the droplet size could improve the surface finish of parts produced in a vertical orientation, as seen previously for fused deposition modeling (FDM) [3].

Fig. 7a illustrates the mean CIEXYZ – Y (luminance) at specular ($\theta_{r\text{-}S}$) and near-to-specular ($\theta_{r\text{-}S} \pm 4°$) angles from 18 geometries for each, associated with luminance results in Figs. 6 and A1. The maximum $\bar{Y}$ at specular angles could be found for BO 0° by 1600.43 ± 924.31, 1410.02 ± 843.26, 1399.56 ± 807.55, and 1376.93 ± 793.8 for CMYK colors, respectively. On the other hand, vertical printing (BO 90°) resulted in the lowest luminances at specular angles by 273.56 ± 166.87, 78.65 ± 42.92, 136.67 ± 55.97, and 174.36 ± 111.41 for CMYK, respectively. The standard deviation followed the same trend.

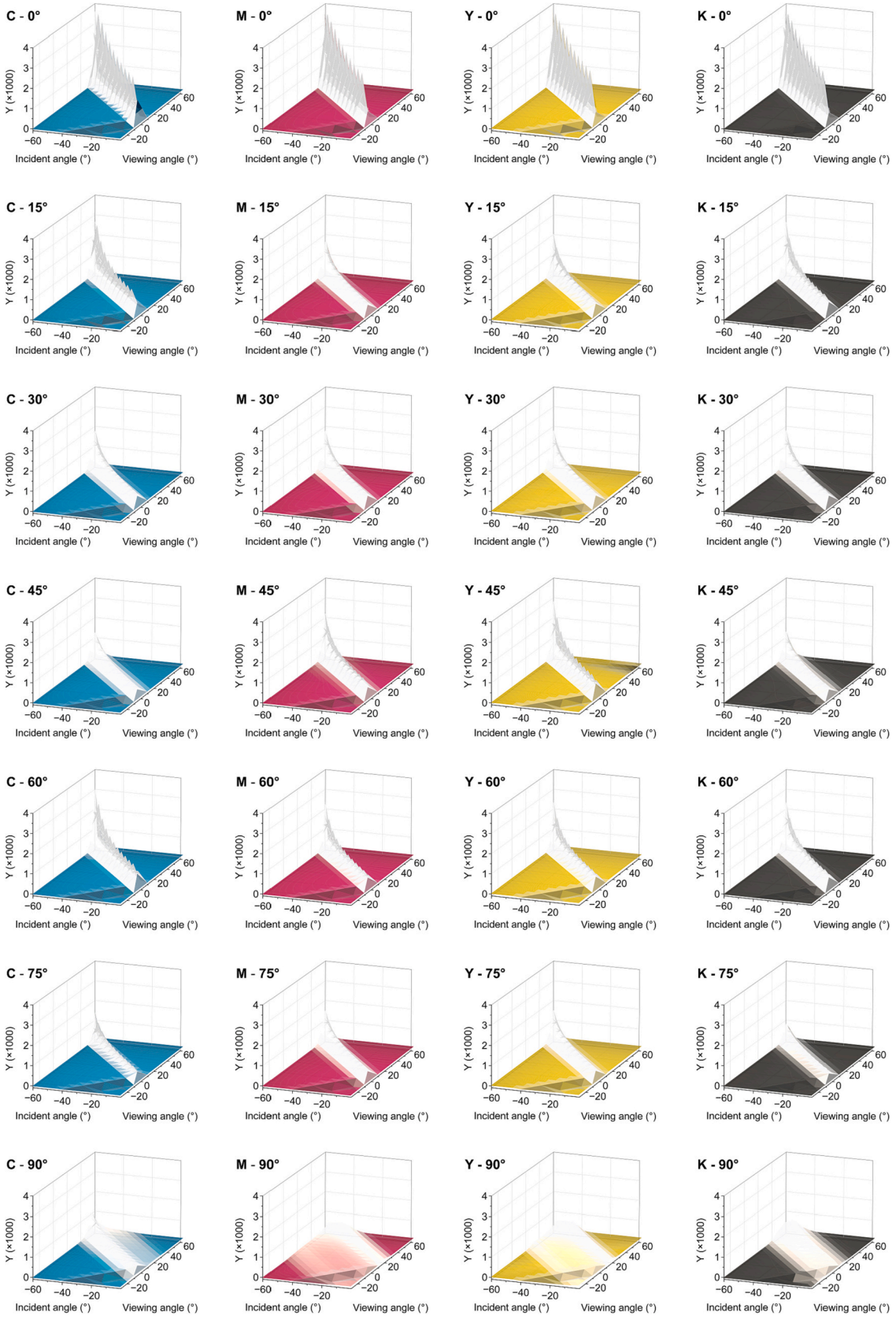

Fig. 5. Surface plot of luminance (Y) of the CMYK resins test sample manufactured at different build orientations. Colors represent the corresponding sRGB hues.

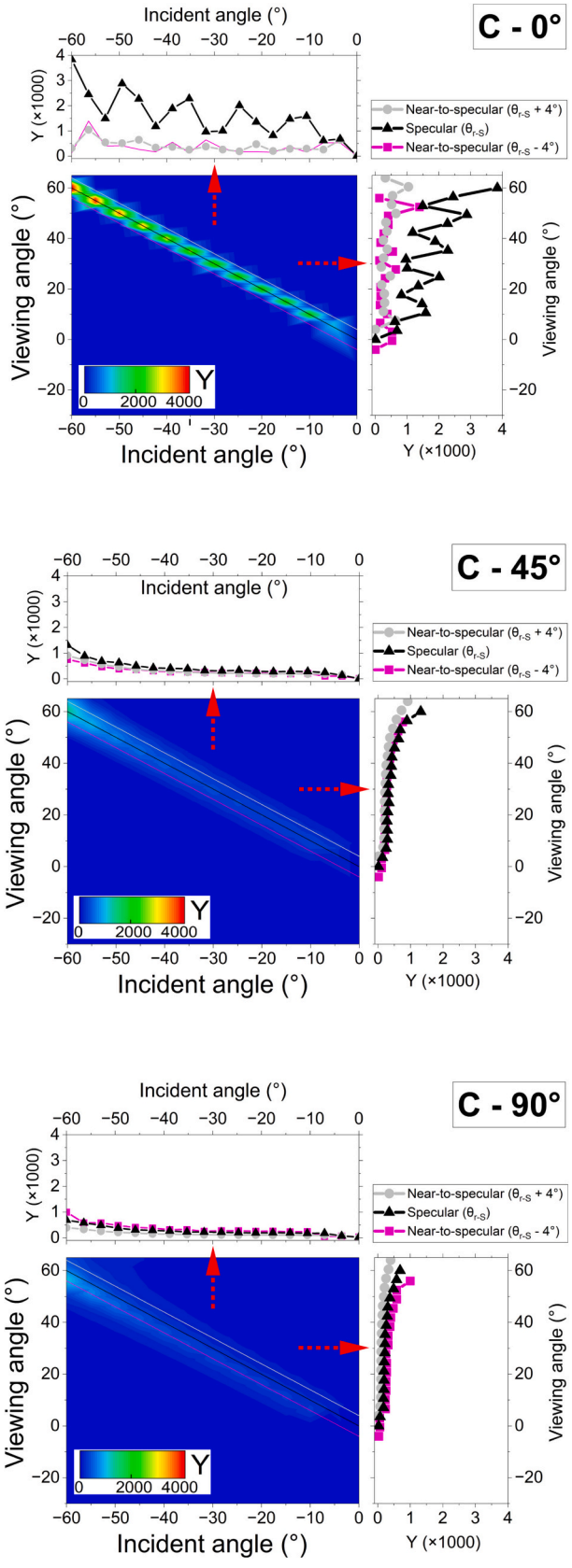

Fig. 6. Luminance Y distribution contour plots for cyan color at BOs 0°, 45°, and 90°. The top and right graphs for each depict the projection of luminance over the incident and viewing angles. (For interpretation of the references to color in this figure legend, the reader is referred to the web version of this article.)

Although increasing BO in most cases resulted in lower luminances, BO 45° and 60° exhibit different behavior depending on the color. In the case of BO 60°, for instance, the luminance for the cyan color was considerably high (1011.95 ± 683.7) compared to BO 45°. As well, near-to-spectral angles for BO 90° displayed greater luminance than specular angles, while in all other BOs, specular angles constantly showed maximum $\bar{Y}$. However, positive near-to-spectral angles ($\theta_{r\text{-}S}$ + 4°) for BO 0° showed higher levels of luminances, and standard deviations (SD) were recorded for magenta, yellow, and black compared to cyan. In the case of specular reflection, the converse behavior was observed for CMYK photo resins. This may be due to multiple factors, including textured surfaces, pigmentation, and uncertainties related to layers deposited at horizontal surfaces, which were observed generally to be more specular at BO 0°. Compared to the other photo resins, cyan photo resin exhibits more excellent specular reflection at BO 0°. The asymmetrical distribution of luminances can be observed in Fig. 7b, revealing both the effect of build orientation and textured surfaces in the employed MJT machine. In this case, it can be related to the rotary build platform and the formation of curvature in layers on the textured surfaces, as previously discussed for this 3D printer [3,15]. Accordingly, it can be seen that negative studied near-to-spectral angles ($\theta_{r\text{-}S}$ - 4°) showed higher CIEXYZ – Y compared to the positive angles because of the orientation of microsurfaces on the manufactured objects [3].

Effective reflectance measurement is crucial for both on-line and off-line appearance measurement. Both on-line appearance measurement during the printing process and off-line appearance measurement of the final product have their own characteristics. On-line measurements must be able to consider any changes in the printing process, such as changes in temperature or humidity, which can affect the final appearance of the object [40]. On the other hand, the off-line measurements employed in this work allow for a more comprehensive analysis of the appearance of the printed item. In particular, BRDF acquisition would be affected by variations in glossiness and transparency caused by environmental agents [52], such as the tendency to water molecules absorption in 3D-printed structures [53], as they are intended to have a higher real surface area than polished objects. Consequently, complex geometric designs and varied microsurfaces result in shadows and highlight fluctuations that pose a challenge to the reflectance capture process.

RDA can provide valuable insights into the relative importance of studied factors and how they interact with each other to influence the appearance characteristics of 3D-printed objects [54]. An RDA plot for Y results is shown in Fig. 8a, which includes vectors representing θ_i and θ_r (observed variables), as well as associated BOs (explanatory labels in Fig. 8b). Since principal component 1 (PC1) represents 99.24 % of the cumulative eigenvalue, a linear correlation between the variables, including measurement geometry and build orientation, could be signified.

The variation in BOs was positively correlated with θ_r, whereas θ_i variation showed a weaker and negative correlation. It can be explained by the alignment of all build orientation vectors toward θ_r, and the opposite direction of θ_i with a shorter vector. Moreover, the vector associated with a BO 90° was assigned to positive PC2, while the remaining vectors were assigned to negative PC2. In other words, printing vertically appeared differently from printing tilted surfaces. This suggests that the build orientation BOs play a critical role in determining the characteristics of the 3D-printed objects in this study. Furthermore, this indicates that the effect of additional factors other than BO variations, including resin colors, was negligible. Appendix B provides complementary data on the RDA results.

PCA scores are presented in Fig. 9, illustrating the relationship between the θ_i and θ_r and the corresponding PCA scores. The sizes of the points on the graph indicate their corresponding PCA scores, with larger points indicating higher scores distributed mainly around −60°:60°. Similar to the observed trends in Figs. 5 and 6, PCA and CIEXYZ – Y demonstrated ties in terms of surface appearance and texture. However,

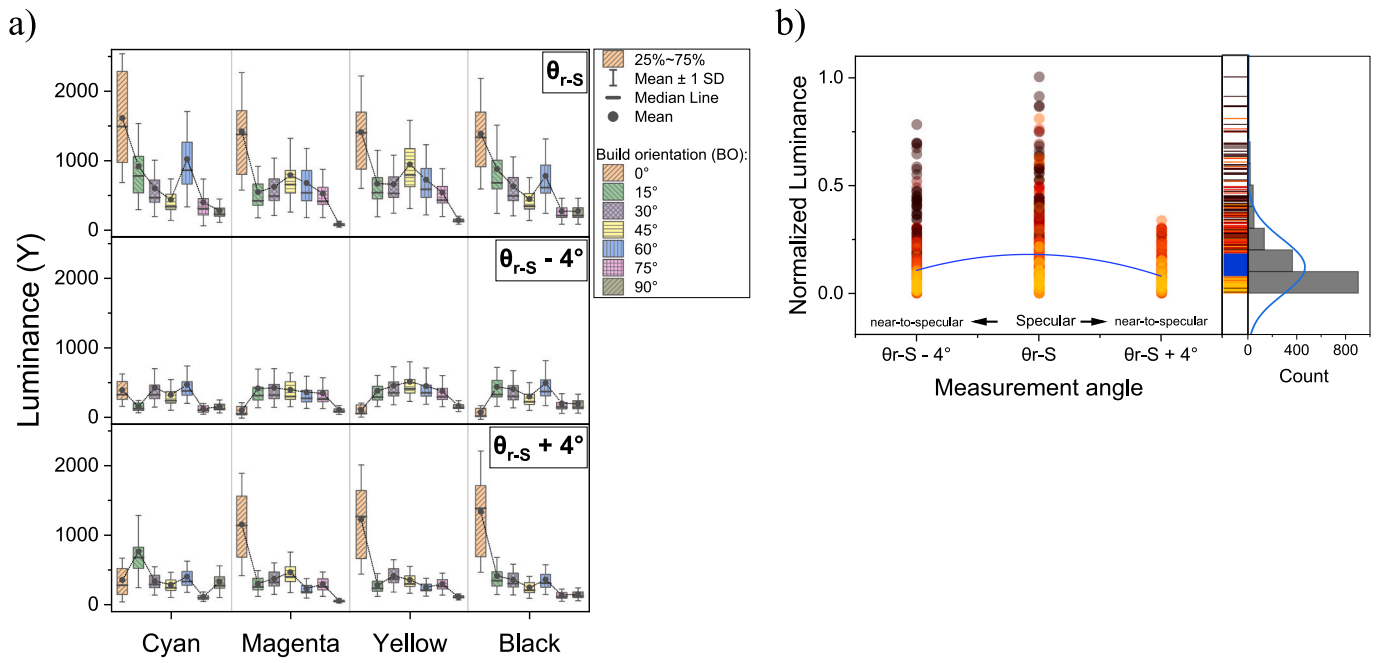

Fig. 7. a) The variation of luminance (CIEXYZ – Y) at specular ($\theta_{r\text{-}S}$) and near-to-specular ($\theta_{r\text{-}S} \pm 4°$) angles considering BO, and b) normalized luminances, histograms, and the corresponding distribution curve.

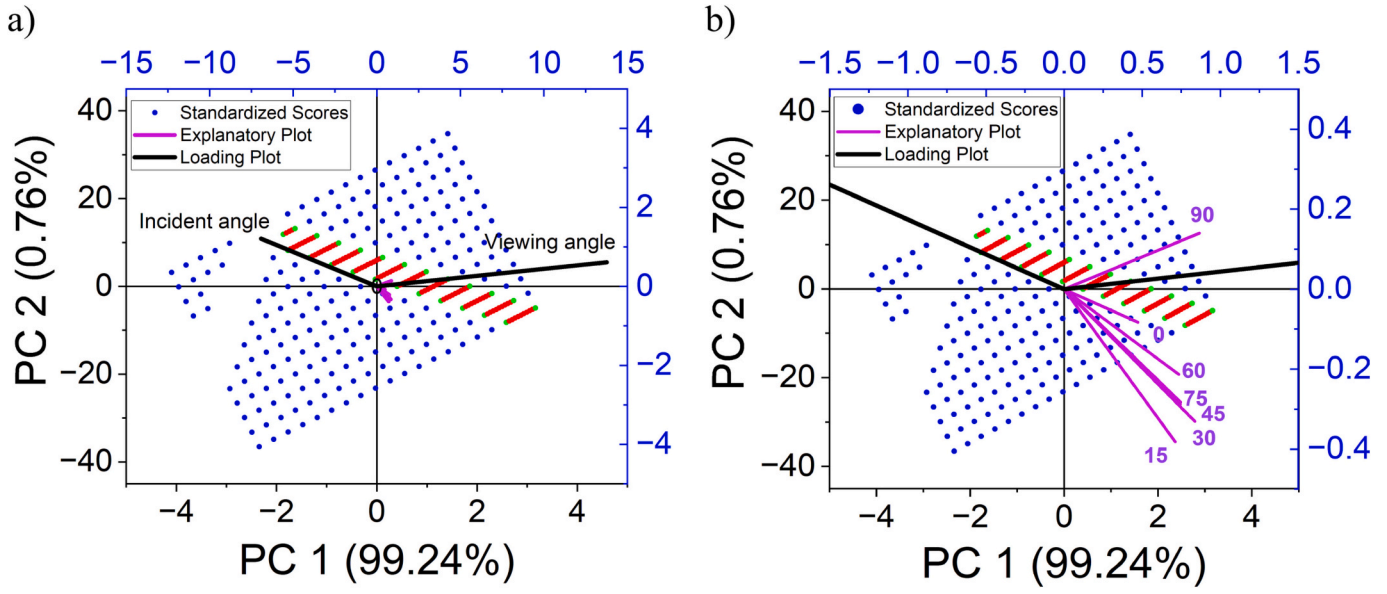

Fig. 8. a) RDA ordination diagram (triplot) of CMYK specimens and b) the corresponding enlarged (10X) triplot considering the explanatory vectors related to the build orientations. The red points represent specular and near-to-specular scores for luminance Y, and the blue points represent the remaining scores. (For interpretation of the references to color in this figure legend, the reader is referred to the web version of this article.)

BO 90° represented shifted results to higher viewing angles due to different textures. Contrary to specular reflection for other BOs, vertical BO demonstrated diffuse reflectance and a more expansive near-to-specular reflectance zone. PCA for spectral data indicated a cumulative percentage of eigenvalues between 97.2 % and 100 % for PC1. It suggests that all the variability in the spectral data could be explained by PC1, and the spectral data for each BRDF measurement batch were linearly correlated.

Limited measurement geometries, mainly within the specular region, could contribute the most to BRDF estimation using the measured bidirectional reflectance. The number of crucial geometries ranged from 12 to 14 pairs of the θ_i and θ_r angles out of the 328 measurement pairs. The bidirectional reflectance measurement process may be optimized for these geometries compared to measuring all possible directions. This would result in a quicker and cost-effective method for measuring the bidirectional reflectance of these materials that can be used for reflectance modeling. Complementary data on the pulse integration results and PCA are listed in Appendix C.

4. Conclusions

Bidirectional reflectance measurements are crucial for understanding the 3D-printed surface texture and appearance. This study evaluated the light reflection on the MJT surfaces using the bidirectional

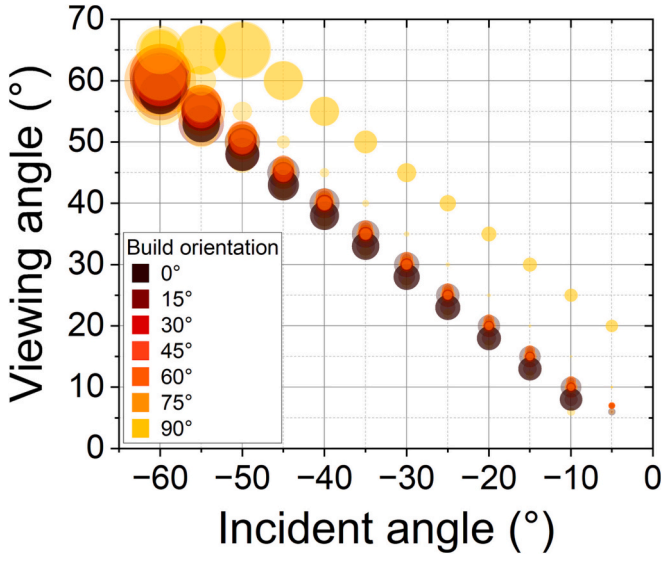

Fig. 9. PCA-based representation of the most prominent measurement angles. Point sizes correspond to standardized PC1 scores.

reflectance measured using a gonio-spectrophotometer. Build orientation can significantly affect the surface texture and roughness of parts produced using the material jetting 3D printing process. According to the results, the combination of a wrong orientation can result in poor accuracy. The texture and surface roughness study revealed a higher build orientation resulted in higher surface roughness, particularly for vertical 3D-printed surfaces. When parts were printed horizontally, the layers of material were deposited on top of one another, resulting in a more uniform surface texture. Alternatively, printed in a vertical orientation, the layers were deposited at an angle, which resulted in an irregular surface texture, especially for BOs of 90°.

In addition, the results indicated that the orientation of the object results in hue and chroma variation, particularly for cyan and magenta resins, compared to yellow and black. The orientation of the build during printing also affects the quality of the 3D-printed part. As a result of the high-speed technology of MJT, large volumes of material can be jetted simultaneously, but a wrong orientation can lead to a decrease in print accuracy. RDA and PCA techniques allowed for identifying significant spectral bands or wavelengths that contributed more to the change in reflectance, as well as the relationship between different variables, such as build orientation and surface reflectance. PCA results suggested that a few illumination and viewing directions were critical for the accurate BRDF estimation. Incorporating luminance distribution (CIEXYZ – Y) and PCA scores of reflectances provided a better understanding of 3D-printed surface appearance attributes like texture and roughness and can lead to better 3D print process optimization. As opposed to specular reflection for other BOs, vertical BOs demonstrated diffuse reflectance and a more expansive near-to-specular reflectance zone.

The choice of model for understanding the interaction of light with materials in AM depends on the properties of the material and the application requirements. It may be more accurate to model translucent or transparent materials or materials that scatter light in all directions with a spatially varying BRDF and/or a BSSRDF model. The BRDF model, however, remains the most popular model to model surface reflectance due to its computational efficiency and suitability for modeling surfaces with specular reflection.

To achieve a full and reliable color accuracy assessment, it is critical to consider various issues when assessing the appearance of 3D-printed color items. On-line measurements are prone to errors because of the dynamic nature of the printing process and process parameters. Another concern is the calibration and precision of measurement instruments to provide accurate appearance measurements. The main factors contributing to measurement errors and discrepancies include illumination, device variability, and color interpretation algorithms. In off-line measurement approach, due to post-production issues such as the aging of samples and defects caused by storage and handling, obtaining the accurate color of a 3D object after printing could be more sophisticated. By considering the specific requirements of the printing process and the appearance characteristics of the printed objects, regardless of the on-line or off-line measurement method, it is possible to reach a more generalized and accurate measurement method.

For future studies, optimizing primary processing parameters and accurately measuring appearance attributes are critical to improving surface quality in MJT technology. It would be vital to evaluate and compare the use of more complex reflectance models like the svBRDF, BSSRDF, and bidirectional transmittance distribution function (BTDF). Moreover, combining materials improvement with targeted appearance attributes of 3D structures opens unprecedented opportunities for further application of AM in the industry. Due to the wide range of materials used in 3D printing, such as metals and ceramics, it is essential to assess whether current measurement methods are effective for textured surfaces. Although most appearance measurements can be conducted following CIE recommendations for various surfaces, further research is required to adjust the measurement workflow for non-resin 3D-printed parts. It is essential for comprehensive color appearance measurement in 3D printing to understand the potential limitations and modifications needed for different material types.

Author agreement

CRediT authorship contribution statement

Ali Payami Golhin: Conceptualization, Methodology, Investigation, Data curation, Formal analysis, Visualization, Writing – original draft, Writing – review & editing. **Aditya Suneel Sole:** Conceptualization, Formal analysis, Writing – review & editing, Supervision. **Are Strandlie:** Writing – review & editing, Supervision, Project administration, Funding acquisition.

Declaration of competing interest

Ali Payami Golhin reports financial support, and article publishing charges were provided by Horizon 2020 (EU) ApPEARS-ITN project [grant No. 814158].

Data availability

The main part of the raw/processed data required to reproduce these findings is available at doi:10.5281/zenodo.7716929.

The rest cannot be shared at this time as the data also forms part of an ongoing study.

Acknowledgments

This work was supported by the ApPEARS-ITN project funded by the European Union's H2020 research and innovation program under the Marie Skłodowska-Curie grant agreement No. 814158. The authors appreciate the support provided by Dr. Andreas Kraushaar (Fogra, Germany) and Donatela Saric (NTNU & Fogra) for the BRDF and roughness measurement.

Appendix A. Supplementary data

Supplementary data to this article can be found online at https://doi.org/10.1016/j.jmapro.2023.09.016.

References

[1] Yuan J, Chen G, Li H, et al. Accurate and computational: a review of color reproduction in full-color 3D printing. Mater. Des. 2021;209:1–17. https://doi.org/10.1016/j.matdes.2021.109943.
[2] Golhin AP, Tonello R, Frisvad JR, et al. Surface roughness of as-printed polymers: a comprehensive review. Int J Adv Manuf Technol 2023;127:987–1043. https://doi.org/10.1007/s00170-023-11566-z.
[3] Golhin AP, Strandlie A. Appearance evaluation of digital materials in material jetting. Opt Lasers Eng 2023;168:107632. https://doi.org/10.1016/j.optlaseng.2023.107632.
[4] Yao D, Yuan J, Tian J, et al. Pigment Penetration Characterization of Colored Boundaries in Powder-Based Color 3D Printing15; 2022. https://doi.org/10.3390/ma15093245.
[5] He J, Lv X. Structural color printing and evaluation based on 3D printing. Pigment Resin Technol 2023. https://doi.org/10.1108/PRT-10-2022-0120. ahead-of-print.
[6] Sugavaneswaran M, Arumaikkannu G. Analytical and experimental investigation on elastic modulus of reinforced additive manufactured structure. Mater. Des. 2015;66:29–36. https://doi.org/10.1016/j.matdes.2014.10.029.
[7] Eren O, Sezer HK, Yalçın N. Effect of lattice design on mechanical response of PolyJet additively manufactured cellular structures. J Manuf Process 2022;75:1175–88. https://doi.org/10.1016/j.jmapro.2022.01.063.
[8] Khoo ZX, Teoh JEM, Liu Y, et al. 3D printing of smart materials: a review on recent progresses in 4D printing. Virtual Phys Prototyping 2015;10:103–22. https://doi.org/10.1080/17452759.2015.1097054.
[9] Payami Golhin A, Strandlie A, John Green P. The influence of wedge angle, feedstock color, and infill density on the color difference of FDM objects. J Imaging Sci Technol 2021;65:1–15. https://doi.org/10.2352/J.ImagingSci.Technol.2021.65.5.050408.
[10] Frisvad JR, Jensen SA, Madsen JS, et al. Survey of models for acquiring the optical properties of translucent materials. In: Computer Graphics Forum. Wiley Online Library; 2020. p. 2. https://doi.org/10.1111/cgf.14023.
[11] L'éclairage CID. Colorimetry in CIE 015:2004. In: Commission Internationale de l'Éclairage; 2004. p. 1–82.
[12] Sole A, Guarnera GC, Farup I, et al. Measurement and rendering of complex non-diffuse and goniochromatic packaging materials. Vis Comput 2021;37:2207–20. https://doi.org/10.1007/s00371-020-01980-9.
[13] Sole A, Farup I, Nussbaum P. Evaluating an image based multi-angle measurement setup using different reflection models. IS and T International Symposium on Electronic Imaging Science and Technology 2017. https://doi.org/10.2352/ISSN.2470-1173.2017.8.MAAP-280.
[14] Wang L, Yuan J, Wu Q, et al. Developing a Quality Evaluation System for Color Reproduction of Color 3D Printing Based on MATLAB Multi-Metrics16; 2023. p. 2424.
[15] Payami Golhin A, Sole AS, Strandlie A. Color appearance in rotational material jetting. Int J Adv Manuf Technol 2023;124:1183–98. https://doi.org/10.1007/s00170-022-10536-1.
[16] Hunt RWG, Pointer MR. Measuring Colour. John Wiley & Sons; 2011.
[17] Serrano A, Chen B, Wang C, et al. The Effect of Shape and Illumination on Material Perception: Model and Applications40; 2021. https://doi.org/10.1145/3450626.3459813.
[18] Reichel S, Blankenbach K, Späth F, et al. Improved light scattering characterization by BSDF of automotive interior and 3D printed materials. Proceedings of SPIE - The International Society for Optical Engineering 2021. https://doi.org/10.1117/12.2578150.
[19] Luongo A, Falster V, Doest MB, et al. Microstructure control in 3D printing with digital light processing. Comput Graph Forum 2020;39:347–59. https://doi.org/10.1111/cgf.13807.
[20] Shi W, Zheng J, Li Y, et al. Measurement and Modeling of Bidirectional Reflectance Distribution Function (BRDF) on Cutting Surface Based on the Coaxial Optical Microscopic Imaging170; 2018. p. 278–86. https://doi.org/10.1016/j.ijleo.2018.04.111.
[21] Guarnera D, Guarnera GC, Ghosh A, et al. BRDF representation and acquisition. In: Computer Graphics Forum. Wiley Online Library; 2016. p. 2. https://doi.org/10.1111/cgf.12867.
[22] Kumar H, Ramkumar J, Venkatesh K. Surface texture evaluation using 3D reconstruction from images by parametric anisotropic BRDF. Measurement 2018;125:612–33. https://doi.org/10.1016/j.measurement.2018.04.090.
[23] Rouiller O, Bickel B, Kautz J, et al. 3D-printing spatially varying BRDFs. IEEE Comput Graph Appl 2013;33:48–57. https://doi.org/10.1109/MCG.2013.82.
[24] D'eon E, Irving G. A quantized-diffusion model for rendering translucent materials. ACM Trans Graph 2011;30:1–14. https://doi.org/10.1145/2010324.1964951.
[25] Haindl M, Filip J. Representation in Visual Texture Springer 2013:9–22.
[26] Hullin MB, Ihrke I, Heidrich W, et al. State of the art in computational fabrication and display of material appearance. In: Eurographics Annual Conference (STAR); 2013.
[27] Galati M, Minetola P. On the Measure of the Aesthetic Quality of 3D Printed Plastic Parts14; 2020. p. 381–92. https://doi.org/10.1007/s12008-019-00627-x.
[28] Serrano A, Chen B, Wang C, et al. The Effect of Shape and Illumination on Material Perception: Model and Applications40; 2021. https://doi.org/10.1145/3450626.3459813. Article 125.
[29] Nicodemus FE, Richmond JC, Hsia JJ, et al. Geometrical Considerations and Nomenclature for Reflectance. 1977.
[30] Habib ST, Green PJ, Nussbaum P. Estimation of BRDF measurements for printed colour samples, in 29th color and imaging conference final program and proceedings. Society for Imaging Science and Technology 2021:123–8. https://doi.org/10.2352/issn.2169-2629.2021.29.123.
[31] Elkhuizen WS, BaJ Lenseigne, Baar T, et al. Reproducing oil paint gloss in print for the purpose of creating reproductions of old masters. In: Proceedings of SPIE - The International Society for Optical Engineering; 2015. https://doi.org/10.1117/12.2082918.
[32] Arteaga Y, Marchioni D, Courtier S, et al. Appearance-based evaluation of varnish removal methods in gilded surfaces. Herit Sci 2023;11:31. https://doi.org/10.1186/s40494-023-00868-w.
[33] Sole A, Farup I, Nussbaum P, et al. Bidirectional reflectance measurement and reflection model fitting of complex materials using an image-based measurement setup. J Imaging 2018;4:1–16. https://doi.org/10.3390/jimaging4110136.
[34] Ulu FI, Mohan RV. Voxel and stereolithographic digital design framework in additive manufacturing: effects in a PolyJet printing process and relevant digital solutions. Prog Addit Manuf 2021;6:653–62. https://doi.org/10.1007/s40964-021-00186-2.
[35] Goh GD, Sing SL, Lim YF, et al. Machine learning for 3D printed multi-materials tissue-mimicking anatomical models. Mater. Des. 2021;211:1–11. https://doi.org/10.1016/j.matdes.2021.110125.
[36] Calignano F, Giuffrida F, Galati M. Effect of the build orientation on the mechanical performance of polymeric parts produced by multi jet fusion and selective laser sintering. J. Manuf. Process. 2021;65:271–82. https://doi.org/10.1016/j.jmapro.2021.03.018.
[37] Taufik M, Jain PK. Laser assisted finishing process for improved surface finish of fused deposition modelled parts. J Manuf Processes 2017;30:161–77. https://doi.org/10.1016/j.jmapro.2017.09.020.
[38] Hanon MM, Ghaly A, Zsidai L, et al. Tribological characteristics of digital light processing (DLP) 3D printed graphene/resin composite: influence of graphene presence and process settings. Mater Des 2022;218:1–17. https://doi.org/10.1016/j.matdes.2022.110718.
[39] Zhu Z, Majewski C. Understanding pore formation and the effect on mechanical properties of high speed sintered polyamide-12 parts: a focus on energy input. Mater. Des. 2020;194:1–16. https://doi.org/10.1016/j.matdes.2020.108937.
[40] Payami Golhin A, Srivastava C, Tingstad JF, et al. Additive manufacturing of multilayered polymer composites: Durability assessment. In: Proceedings of the 20th European Conference on Composite Materials-Composites Meet Sustainability (Vol 1–6). Lausanne, Switzerland: EPFL Lausanne, Composite Construction Laboratory Switzerland; 2022. https://doi.org/10.5075/epfl-298799_978-2-9701614-0-0.
[41] Khoshkhoo A, Carrano AL, Blersch DM. Effect of build orientation and part thickness on dimensional distortion in material jetting processes. Rapid Prototyping J 2018;24:1563–71. https://doi.org/10.1108/RPJ-10-2017-0210.
[42] Gao H, Yang Z, Lin WS, et al. The effect of build orientation on the dimensional accuracy of 3D-printed mandibular complete dentures manufactured with a multijet 3D printer. J Prosthodont 2021;30:684–9. https://doi.org/10.1111/jopr.13330.
[43] Das SC, Ranganathan R, Murugan N. Effect of build orientation on the strength and cost of PolyJet 3D printed parts. Rapid Prototyping J. 2018;24:832–9. https://doi.org/10.1108/RPJ-08-2016-0137.
[44] Zelený P, Šafka J, Elkina I. The mechanical characteristics of 3D printed parts according to the build orientation. Appl Mech Mater 2014:381–6. https://doi.org/10.4028/www.scientific.net/AMM.474.381.
[45] Stratasys. Vero: realistic, multi-color prototypes in less time. In: Stratasys Datasheet; 2022. p. 1–4.
[46] Stratasys.. 3D printing with pantone colors. Stratasys Ltd. 2021:1–6.
[47] Pandey P, Nayak A, Taufik M. Evaluation of Mathematical Models for Surface Roughness Prediction of PolyJet 3D Printed Parts. 2022. https://doi.org/10.1080/2374068X.2022.2097416.

[48] Gülcan O, Günaydın K, Çelik A. Investigation on Surface Roughness of Polyjet-Printed Airfoil Geometries for Small UAV Applications9; 2022. https://doi.org/10.3390/aerospace9020082.
[49] Iso. Geometrical product specifications (GPS) — surface texture: areal — part 2: terms, definitions and surface texture parameters. In: ISO 25178-2:2021. International Organization for Standardization: Geneva, Switzerland; 2021. p. 1–64.
[50] Park JM, Jeon J, Koak JY, et al. Dimensional accuracy and surface characteristics of 3D-printed dental casts. J Prosthet Dent 2021;126:427–37. https://doi.org/10.1016/j.prosdent.2020.07.008.
[51] Témun A, Mattsson L, Heikkilä I. Localizing micro-defects on rough metal surfaces. In: Menz W, Dimov S, Fillon B, editors. 4M 2006 - Second International Conference on Multi-Material Micro Manufacture. Oxford: Elsevier; 2006. p. 169–72.
[52] Payami Golhin A, Srivastava C, Strandlie A, et al. Effects of accelerated aging on the appearance and mechanical performance of materials jetting products. Materials & Design 2023;228:111863. https://doi.org/10.1016/j.matdes.2023.111863.
[53] Chand R, Sharma VS, Trehan R, et al. Investigating the Dimensional Accuracy and Surface Roughness for 3D Printed Parts Using a Multi-Jet Printer. 2022. https://doi.org/10.1007/s11665-022-07153-0.
[54] Lepš J, Šmilauer P. Multivariate Analysis of Ecological Data Using CANOCO. Cambridge university press; 2003.

Ali Payami Golhin received his PhD in Engineering as a Marie Skłodowska-Curie fellow at NTNU - Norwegian University of Science and Technology. His research focuses on the study of the optical properties of structured surfaces. He has a research background in additive manufacturing, optical characterization, tribology, and materials engineering.

Aditya Sole received his doctoral degree from the Department of Computer Science at the Norwegian University of Science and Technology, Gjøvik, Norway in 2019 and currently is working as an Associate Professor at the computer science department at NTNU Gjøvik campus mainly focusing his research on the field of measuring, understanding, and reproduction of visual appearance and 3D printing. He is also involved in MSCA-ITN-ETN funded ApPEARS project as a deputy scientific coordinator and RCN-INTPART funded MANER project as a project manager.

Are Strandlie is a Professor of Physics at NTNU - Norwegian University of Science and Technology. His main research interests are data analysis methods for high-energy physics experiments and numerical methods for material physics. Recently, an increasing interest has emerged within cross-disciplinary topics, such as the link between appearance and material properties.